Global and Planetary Change 143 (2016) 251–261

Contents lists available at ScienceDirect

Global and Planetary Change

journal homepage: www.elsevier.com/locate/gloplacha

Holocene climate change in Newfoundland reconstructed using oxygen isotope analysis of lake sediment cores

Matthew S. Finkenbinder [a,*], Mark B. Abbott [a], Byron A. Steinman [b]

[a] Department of Geology and Environmental Science, University of Pittsburgh, Pittsburgh, PA, USA
[b] Department of Earth and Environmental Sciences and Large Lakes Observatory, University of Minnesota Duluth, Duluth, MN, USA

ARTICLE INFO

Article history:
Received 11 January 2016
Received in revised form 6 May 2016
Accepted 22 June 2016
Available online 25 June 2016

Keywords:
Paleoclimate
Carbonate oxygen isotopes
Open-basin lakes
Holocene
Newfoundland
North Atlantic

ABSTRACT

Carbonate minerals that precipitate from open-basin lakes can provide archives of past variations in the oxygen isotopic composition of precipitation ($\delta^{18}O_{ppt}$). Holocene $\delta^{18}O_{ppt}$ records from the circum- North Atlantic region exhibit large fluctuations during times of rapid ice sheet deglaciation, followed by more stable conditions when interglacial boundary conditions were achieved. However, the timing, magnitude, and climatic controls on century to millennial-scale variations in $\delta^{18}O_{ppt}$ in northeastern North America are unclear principally because of a dearth of paleo-proxy data. Here we present a lacustrine sediment oxygen isotope ($\delta^{18}O$) record spanning 10,200 to 1200 calendar years before present (cal yr BP) from Cheeseman Lake, a small, alkaline, hydrologically open lake basin located in west-central Newfoundland, Canada. Stable isotope data from regional lakes, rivers, and precipitation indicate that Cheeseman Lake water $\delta^{18}O$ values are consistent with the isotopic composition of inflowing meteoric water. In light of the open-basin hydrology and relatively short water residence time of the lake, we interpret down-core variations in calcite oxygen isotope ($\delta^{18}O_{cal}$) values to primarily reflect changes in $\delta^{18}O_{ppt}$ and atmospheric temperature, although other factors such as changes in the seasonality of precipitation may be a minor influence. We conducted a series of climate sensitivity simulations with a lake hydrologic and isotope mass balance model to investigate theoretical lake water $\delta^{18}O$ responses to climate change. Results from these experiments suggest that Cheeseman Lake $\delta^{18}O$ values are primarily controlled by temperature and to a much lesser extent, the seasonality of precipitation. Increasing and more positive $\delta^{18}O_{cal}$ values between 10,200 and 8000 cal yr BP are interpreted to reflect the waning influence of the Laurentide Ice Sheet on atmospheric circulation, warming temperatures, and rapidly changing surface ocean $\delta^{18}O$ from the input of glacial meltwater into the western North Atlantic Ocean. The increasing trend is interrupted by abrupt negative $\delta^{18}O_{cal}$ anomalies at 9700 cal yr BP, associated with a transition to colder sea surface temperatures (SSTs) in the Labrador Sea and renewed Laurentide Ice Sheet retreat, and at 8500 cal yr BP that coincides with a well-established cooling event in the circum-North Atlantic region. After 8000 cal yr BP, $\delta^{18}O_{cal}$ values gradually decrease until 4300 cal yr BP, which reflects a cooling trend related to declining Boreal summer insolation and lower sea surface temperatures in the western North Atlantic Ocean. $\delta^{18}O_{cal}$ becomes slightly more positive from 4300 to 2500 cal yr BP and thereafter declines to the most negative values of the late Holocene by 1200 cal yr BP. The middle to late-Holocene transition at ~4300 cal yr BP corresponds with a shift to wetter conditions in Newfoundland that is also seen in other paleo-proxy records from the region. The discordance between the Cheeseman Lake $\delta^{18}O_{cal}$ record and declining insolation could in part reflect warmer temperatures or an increase (decrease) in warm (cold) season precipitation. Considering evidence from other paleo-records in Newfoundland, we suggest this transition resulted from a change in synoptic scale atmospheric circulation to a configuration similar to the positive mean state phase of the Pacific-North American pattern. Proxy evidence from Cheeseman Lake therefore supports the idea that a substantial climatic change occurred during the middle to late-Holocene transition (between ~5000 to ~4000 cal yr BP) in northeastern North America.

* Corresponding author.
E-mail address: msf34@pitt.edu (M.S. Finkenbinder).

http://dx.doi.org/10.1016/j.gloplacha.2016.06.014
0921-8181/

1. Introduction

The oxygen isotopic composition of precipitation ($\delta^{18}O_{ppt}$) is an effective tracer of the global hydrologic cycle (Gat, 1995; Araguás-Araguás et al., 2000). $\delta^{18}O_{ppt}$ is controlled by the initial isotopic composition of water vapor at the moisture source and fractionation processes that occur during rainout and subsequent evaporation (Dansgaard, 1964; Rozanski et al., 1992). Reconstructions of paleo $\delta^{18}O_{ppt}$ from ice cores (e.g. Dansgaard et al., 1985; NGRIP, 2004), speleothems (e.g. Ersek et al., 2012), tree rings (e.g. Bale et al., 2010), and lake sediments (e.g. Edwards et al., 1996) can therefore provide valuable information on the paleohydrological and paleoclimatic conditions of the Holocene. For instance, high-resolution $\delta^{18}O_{ppt}$ records from Greenland ice cores reveal substantial changes in atmospheric temperature and snowfall accumulation over the current interglacial (Grootes and Stuiver, 1997), as well as the occurrence of early Holocene abrupt climate events at 9300 and 8200 calendar years before present (cal yr BP) that have been linked to catastrophic drainage of proglacial lakes (Barber et al., 1999) and short-lived cooling events (Alley et al., 1997; Yu et al., 2010; Daley et al., 2011). While highly informative, the Greenland $\delta^{18}O_{ppt}$ records largely provide information on a restricted geographic area (Grootes and Stuiver, 1997; NGRIP, 2004; Vinther et al., 2009), and much less is known about spatial variability in paleo-$\delta^{18}O_{ppt}$ across the greater North Atlantic region over the Holocene, particularly in the underrepresented Atlantic Canadian provinces (Daley et al., 2009).

Here we present a lacustrine oxygen isotope ($\delta^{18}O$) record from a small, alkaline lake (Cheeseman Lake) located in west-central Newfoundland, Canada spanning the period 10,200 to 1200 cal yr BP. We analyzed the stable isotope composition (δD and $\delta^{18}O$) of surface water samples, instrumental climate data from a proximal weather station, and monthly precipitation δD and $\delta^{18}O$ data from a Canadian Network of Isotopes in Precipitation (CNIP) station to investigate modern lake-catchment hydrologic and water isotope relationships. To provide a framework for interpreting the Cheeseman Lake $\delta^{18}O$ record, we employed a coupled hydrologic and water isotope mass balance model (Steinman et al., 2010) to assess the sensitivity of the lake to hydroclimate forcing (Steinman and Abbott, 2013). We interpret the Cheeseman Lake $\delta^{18}O$ record in the context of Greenland ice core $\delta^{18}O$ data, near shore marine records, and several terrestrial hydroclimate records from Newfoundland to evaluate the underlying causes of centennial to orbital scale climate variability in the North Atlantic region during the Holocene.

2. Site location and regional setting

Cheeseman Lake (informal name; 49.351° N, 57.603° W, 180 m asl) is a small (0.2 km^2), alkaline, open-basin lake located near the coast of west-central Newfoundland (Fig. 1). The lake is elliptical in shape, and the small (1.9 km^2) surrounding watershed (Supplemental Fig. 1) is characterized by moderately steep slopes along much of the shoreline. The lake receives inflow from a stream on the southwest shore and drains to Lomond River through an outlet stream on the northeast side. The maximum water depth is 4.1 m near the geometric center of the basin. The catchment contains second-growth forests that are characterized by a Dryopteris-Hylocomium-Balsam Fir forest type (South, 1983).

The lake and surrounding area is located in the West Coast Calcareous Uplands physiographic province, characterized by hilly terrain and irregular topography (South, 1983). Alkaline ponds that precipitate carbonate minerals, similar to Cheeseman Lake, are a common feature of the province. Bedrock geology in the catchment consists of Cambrian to Ordovician age limestone, dolostone, and shale (Colman-Sadd et al., 2000). Surficial geology in the immediate area is till veneer, which is composed of a thin (< 1.5 m) discontinuous sheet of lodgment till (Liverman and Taylor, 1990). The Island of Newfoundland was covered by the Laurentide Ice Sheet during the last glacial period (Dyke and Prest, 1987). Humber River Gorge and the lower Deer Lake valley, located ~30 km southeast of Cheeseman Lake, was deglaciated by 14,100 cal yr BP (median age; 13,800 to 14,600 cal yr BP 2σ uncertainty) (12,220 ± 90 ^{14}C yr BP) (Batterson and Catto, 2001). Post-glacial isostatic depression resulted in higher relative sea level in west-central Newfoundland in the latest Pleistocene (Batterson and Catto, 2001) and presumably an unstable land surface. Cheeseman Lake was not inundated by higher sea levels during deglaciation; however, the lake and catchment were presumably influenced by general landscape instability during the rapid isostatic adjustment that followed deglaciation.

The climate of Newfoundland is principally controlled by the marine influence of the Gulf of St. Lawrence and Atlantic Ocean along with the North Atlantic Oscillation (NAO) (Ullah, 1992), a hemisphere-wide

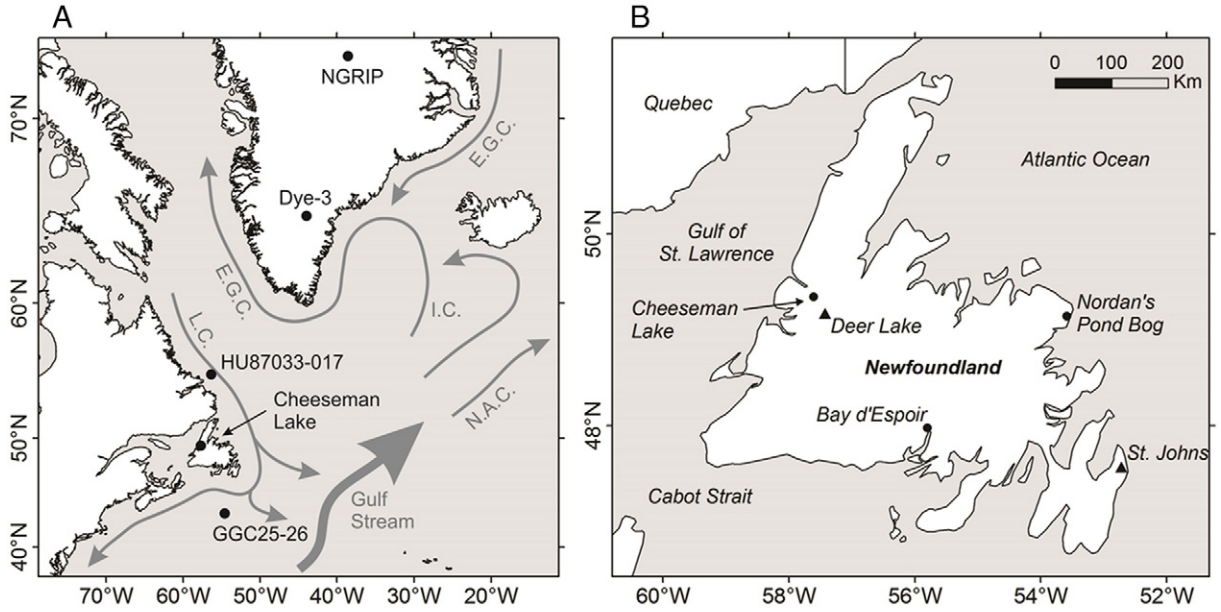

Fig. 1. a) Map of the western North Atlantic region showing modern surface ocean currents and sites mentioned in the text. Ocean currents include, N.A.C. – North Atlantic Current, E.G.C. – East Greenland Current, I.C. – Irminger Current, and L.C. – Labrador Current. b) Map of Newfoundland with Cheeseman Lake (informal name) and other sites mentioned in the text.

atmospheric circulation pattern (closely related to the Northern Annular Mode) that influences the strength of zonal atmospheric flow. The Labrador Current, which transports cold, ex-Arctic waters along the eastern continental margin as well as the northeastward flowing North Atlantic Current (Fig. 1) produce Newfoundland's generally mild winters and cool summers (Ullah, 1992). Warmer temperatures typically occur in the south of Newfoundland due to the absence of offshore sea ice (Ullah, 1992). Climate data from Deer Lake (Fig. 1) indicate average winter (January–February-March) and summer (June–July-August) temperatures of −6.8 °C and 15.0 °C (Supplemental Fig. 2), respectively . Precipitation is generally distributed evenly over the year, with slightly lesser amounts during the late winter/early spring, but otherwise there is not a distinct wet season (Supplemental Fig. 2). The NAO, defined by the pressure difference between the Azores High and the Icelandic Low pressure systems, influences atmospheric circulation and temperatures across the Northern Hemisphere, particularly during the winter (Hurrell and Deser, 2009). In Newfoundland, the positive phase of the NAO index is associated with below average winter temperatures (and vice versa) (Supplemental Fig. 3) (Banfield and Jacobs, 1998). Cold-season precipitation and the NAO index are not significantly correlated (Supplemental Fig. 3) (Banfield and Jacobs, 1998).

3. Methods

3.1. Sediment coring and sample collection

Sediment cores were collected from the center of Cheeseman Lake in August 2012. A surface core (A-12) with an undisturbed sediment-water interface was recovered from 3.5 m water depth using a polycarbonate tube attached to a rod-driven piston corer. The flocculate upper 32 cm of the surface core was extruded in the field at 1 cm intervals into sterilized whirl-pak bags. Multiple overlapping 1 m cores were recovered from an adjacent core site (B-12) in 4.1 m water depth using a Livingstone corer.

Water samples for oxygen ($\delta^{18}O$) and hydrogen (δD) isotope analyses were collected in 30 ml polyethylene bottles from the surface water of regional lakes and streams in August 2012. Measurements are reported in standard delta (δ) notation as the per mil (‰) deviation from Vienna Standard Mean Ocean Water (VSMOW). Monthly precipitation $\delta^{18}O$ and δD data from a Canadian Network for Isotopes in Precipitation (CNIP) station at Bay d'Espoir, Newfoundland (Fig. 1) from the period 1997 to 2010 were analyzed to estimate the sensitivity of Cheeseman Lake water isotopes to hydroclimate forcing.

3.2. Lithostratigraphy

Sediment cores were split and described at the Department of Geology and Environmental Science at the University of Pittsburgh. Notable sedimentary structures, grain size, and Munsell color were characterized for each core. All cores were sampled at 1 cm intervals, and dry bulk density was calculated from dry weights of volumetric samples. Loss-on-ignition (LOI) analysis was conducted at 550 °C for 4 h and 1000 °C for 2 h to estimate the weight percent organic matter and total carbonate (Heiri et al., 2001). A composite sediment core sequence was developed using field measurements and by matching visible stratigraphic markers, including laminae and banded features common to overlapping cores, between the A-12 surface core and B-12 Livingstone cores (Fig. 2) (Supplemental Fig. 4).

3.3. Geochronology

Age control was developed using ^{210}Pb dating of surface sediments and Accelerator Mass Spectrometry (AMS) radiocarbon analyses of wood, charcoal, and plant macrofossils (Table 1) (see Supplemental). An age-depth model was created using a cubic spline interpolator with the classical age modeling (CLAM) software v2.2 (Blaauw, 2010). The CLAM analysis performed 1000 age model iterations based on repeated sampling of the calibrated age distributions for each radiocarbon sample to estimate the 'best fit' or weighted mean age for each depth.

3.4. Geochemistry

A total of 5 samples from the composite core were analyzed for X-ray diffraction (XRD) and scanning electron microscopy (SEM) to characterize the carbonate mineralogy at the Materials Micro-Characterization Laboratory at the University of Pittsburgh, Swanson School of

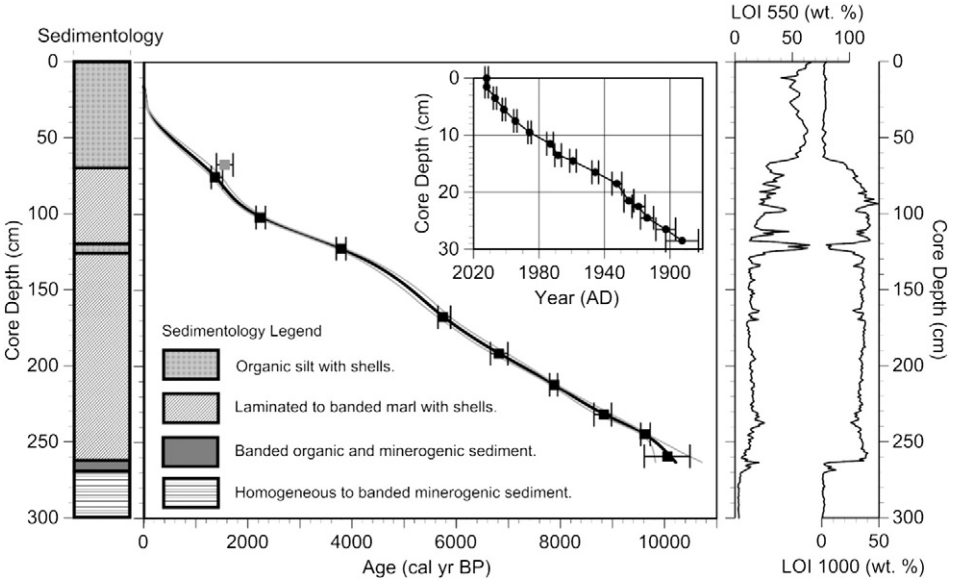

Fig. 2. Stratigraphic column and age model for the Cheeseman Lake core sequence developed from Accelerator Mass Spectrometry radiocarbon and ^{210}Pb dates using a cubic spline interpolation. The radiocarbon dates (squares) are presented as the median calibrated age with the associated 2σ uncertainty for each control point (error bars) and the overall age model (grey lines). The sample at 67.5 cm depth highlighted with a grey square is rejected from the age model. The ^{210}Pb dates (circles) include the 1σ analytical uncertainty derived from the Constant Rate of Supply model calculations. Weight percent organic matter and total carbonate from LOI 550 (wt.%) and LOI 1000 (wt.%) analysis.

Table 1
AMS radiocarbon dates from the Cheeseman Lake core sequence with calibrated 2 sigma error ranges. Ages were calibrated using Calib 7.0 and the IntCAL13 calibration curve (Reimer et al., 2013). The sample highlighted with an asterisk was rejected from the age model, as explained in the main text.

UCIAMS #	Core	Total Depth (cm)	Material	^{14}C age yr BP	± yr	Calib 2σ yr BP
*131,491	A-12 67-68 cm	67.5	plant material	1650	70	1389–1711
131,491	A-12 75-76 cm	75.5	wood	1485	40	1301–1518
116,881	B-12 D1 15 cm	102	wood	2250	20	2159–2339
131,492	B-12 D1 35-36 cm	122.5	wood	3520	35	3698–3887
122,242	B-12 D1 80-81 cm	167.5	wood	5010	45	5651–5895
122,243	B-12 D2 22-23 cm	191.5	charcoal	5980	70	6660–6993
141,393	B-12 D2 43 cm	212	charcoal	7040	35	7795–7947
116,882	B12 D2 62-63 cm	231.5	wood	7955	30	8649–8985
141,394	B-12 D2 76 cm	244.5	charcoal	8680	35	9544–9727
131,493	B12 D2 90 cm	259	wood	8980	150	9614–10,491

Engineering (see Supplemental). The composite core sequence was sampled at continuous 1 cm intervals between 262 and 70 cm for carbonate stable isotope analysis of oxygen ($\delta^{18}O_{cal}$) and carbon ($\delta^{13}C$). Fine-grained (<63 μm) carbonate sediment was prepared for isotope analysis according to standard analytical procedures (see Supplemental). Measurements are reported in standard delta (δ) notation as the per mil (‰) deviation from Vienna Pee Dee Belemnite (VPDB).

3.5. Lake hydrology and isotope modeling

To investigate the sensitivity of the oxygen isotopic composition of Cheeseman Lake water ($\delta^{18}O_{lw}$) to specific climate variables and to develop a quantitative basis for the interpretation of sediment oxygen isotope values, we conducted simulations using a coupled lake hydrologic and isotope mass balance model (Steinman et al., 2010, 2016; Steinman and Abbott, 2013) (see Supplemental). In this study, we utilize the model to characterize the isotopic response of lake water and sedimentary calcite to changes in atmospheric temperature (±1 and ±2 °C) and the seasonality of winter (October to March) and summer (April to September) season precipitation (± 20%). Given the open-basin hydrology of Cheeseman Lake, these climatic variables should primarily control lake geochemical responses to climate forcing. The model consists of a system of four ordinary differential equations that describe two water reservoirs (for lake water balance and catchment-groundwater balance), as well as corresponding isotope mass balance reservoirs, and volumetric fluxes including direct precipitation on the lake, inflow from the catchment-groundwater system, and the subtraction of overflow and lake water evaporation. Steady state simulations were conducted using average monthly climate data from Deer Lake, Newfoundland, precipitation isotope data from the Bay d'Espoir CNIP station in south-central Newfoundland, and gridded climate model reanalysis data (Table 2). The results of sensitivity tests provide support for the interpretation of Cheeseman Lake sediment $\delta^{18}O_{cal}$ values.

4. Results

4.1. Sedimentology and geochemistry

The Cheeseman Lake cores consist of silicate minerogenic and organic sediments from 300 to 263 cm, banded to laminated calcareous sediments with variable organic content from 263 to 70 cm, and organic silty sediments from 70 cm to the core top (Fig. 2; see Supplemental). Powder XRD analysis indicates the primary carbonate mineral present in the cores is calcite (Supplemental Fig. 5), with no other calcite polymorphs (i.e. aragonite) present in the measured samples. SEM analysis further shows the presence of near perfect, rhombic (euhedral) calcite crystal form (Supplemental Fig. 6). Collectively, these results indicate that carbonate minerals within the sediment core are authigenic calcite precipitated from the water column.

4.2. Chronology

The ^{210}Pb inferred CRS age model for the surface sediments indicates that a depth of 28 cm corresponds to the year ~1890 CE (Fig. 2). The 1963 CE peak in ^{137}Cs from atmospheric thermonuclear weapons testing occurs from 11.5 to 14.5 cm, broadly consistent with the CRS inferred age for this interval of 1959 to 1973 CE. The uppermost radiocarbon sample (UCIAMS # 116,880) at 67–68 cm was excluded prior to generating the age model, based on a slight age reversal between the oldest reliable ^{210}Pb date and adjacent radiocarbon sample (UCIAMS # 131,490). The rejected sample appears anomalously old for its stratigraphic position and has a slightly larger analytical uncertainty in comparison to the adjacent date. This sample was an aquatic or submerged macrophyte, which lacked obvious vascular structure indicative of terrestrial plants, that likely incorporated ^{14}C depleted dissolved inorganic carbon, resulting in a dead carbon contribution to the sample. This hypothesis is consistent with core sedimentology that shows the presence of aquatic vegetation

Table 2
Model input and meteorological station data. (a) Deer Lake, Newfoundland Climate Normals 1981–2010 (Environment Canada, 2010). (b) NOAA 20th Century Gridded *Re*-analysis Project data (Compo et al., 2011). (c) Bay d'Espoir, NL monthly mean precipitation isotope values for the period 1997–2010.

Month	Precipitation[(a)] (mm)	Temperature[(a)] (°C)	Relative Humidity (%)[(b)]	Wind Speed (m/s)[(b)]	Incoming Solar rad. (MJ m^{-2} d^{-1})[(b)]	$\delta^{18}O$ (‰)[(c)]	δD (‰)[(c)]
Jan	109.8	−7.2	94.4	6.3	4.7	−12.5	−89.5
Feb	83.5	−8	95.4	5.8	7.8	−11.6	−80.3
Mar	71.7	−4.1	95.0	5.8	11.9	−11.5	−81.5
Apr	70.1	1.9	93.0	5.3	15.6	−9.3	−64.0
May	89.2	7.4	84.7	4.7	19.3	−8.1	−57.9
Jun	88.3	12.2	80.0	4.6	21.1	−7.7	−52.2
Jul	98.5	16.5	80.1	4.7	21.0	−6.7	−46.4
Aug	109.9	16.4	78.6	4.7	18.4	−6.3	−39.9
Sep	106.2	12.3	80.0	5.0	13.2	−8.0	−53.0
Oct	105.7	6.6	85.7	5.5	7.8	−8.2	−54.5
Nov	101.3	1.5	89.4	5.9	4.6	−8.5	−55.2
Dec	97.3	−3.3	93.1	6.2	3.6	−11.7	−79.3

in the upper 70 cm of the composite core (Fig. 2). The age model indicates generally low and variable sedimentation rates between ~0.01 to ~0.04 cm/yr from 259 to 28 cm depth that increase towards the core top (Fig. 2). Carbonate sediments for stable isotope analysis are continuously present between 262 and 70 cm across the interval spanning 10,200 to 1200 cal yr BP (Fig. 2).

4.3. Modern water isotopes

The local meteoric water line (LMWL), developed with monthly average precipitation isotope data from the Bay d'Espoir CNIP station (Table 2), is parallel and offset from the global meteoric water line (GMWL) (Rozanski et al., 1992) (Fig. 3). Cheeseman Lake surface waters ($\delta^{18}O = -9.0‰$, $\delta D = -65.1‰$) plot along the LMWL (Fig. 3), suggesting that lake waters reflect the isotopic composition of precipitation. The average weighted $\delta^{18}O$ of precipitation was calculated by normalizing monthly average precipitation $\delta^{18}O$ from the Bay d'Espoir CNIP station with the monthly proportion of annual precipitation from Deer Lake (Supplemental Fig. 2) and has a value of −9.1‰, similar to the measured lake water value of −9.0‰. Many lakes in the region are substantially influenced by evaporation and have isotope values that define (and therefore plot along) the local evaporation line (LEL) (Fig. 3).

4.4. Carbonate stable isotope measurements

We assign two zones to the calcite $\delta^{18}O$ ($\delta^{18}O_{cal}$) data in order to facilitate discussion (Fig. 4). Zone 1 begins at the transition from minerogenic to carbonate sediments at 262 cm and extends to 213 cm, spanning the interval between 10,200 and 8000 cal yr BP. Cheeseman $\delta^{18}O_{cal}$ values decrease from −10.9‰ to −11.5‰ abruptly between 10,200 and 10,100 cal yr BP (Fig. 4). After 10,100 cal yr BP, $\delta^{18}O_{cal}$ values exhibit centennial variability and increase to −10.0‰ at the Zone 2 boundary (~ 8000 cal yr BP). $\delta^{18}O_{cal}$ values are abbreviated by rapid excursions to more negative values beginning at 9700 and 8500 cal yr BP that persist for ~200 years (Fig. 4). $\delta^{18}O_{cal}$ values increase rapidly from −10.9‰ to −10.0‰ between 8300 and 8000 cal yr BP. Zone 2 extends from 213 cm to 70 cm and spans the interval between 8000 and 1200 cal yr BP. Cheeseman $\delta^{18}O_{cal}$ values gradually decrease with distinct centennial variability from −10.0‰ to −11.1‰ between 8000 and 4300 cal yr BP (Fig. 4). Slightly more positive $\delta^{18}O_{cal}$ values (−10.6‰) occur between 4300 and 2500 cal yr BP. $\delta^{18}O_{cal}$ values are generally lower after 2500 cal yr BP (−11.0‰) with minimal variability until 1200 cal yr BP (Fig. 4). Variations in calcite $\delta^{13}C$, which range between −6.4 and −3.7‰ (VPDB) over the record, are distinct in comparison with changes in $\delta^{18}O$ (Fig. 4).

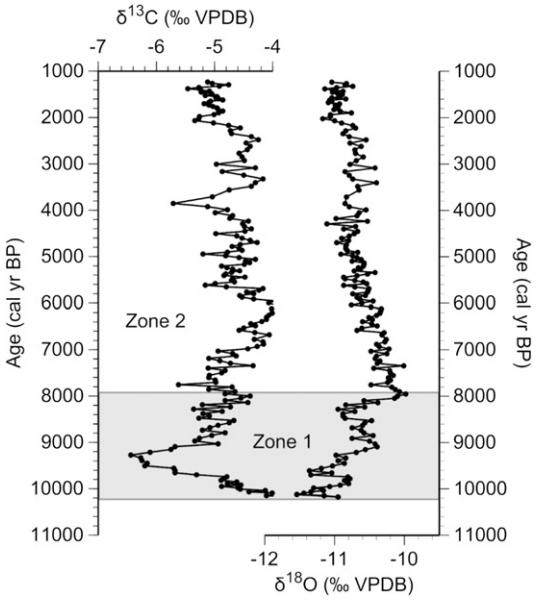

Fig. 4. Cheeseman Lake sediment calcite stable isotope data.

4.5. Model calibration and sensitivity tests

The steady-state model simulation produced a theoretical summer (June–August) $\delta^{18}O_{cal}$ value of −10.71‰, which is similar to the measured $\delta^{18}O_{cal}$ value of −11.04‰ at ~1200 cal yr BP. Atmospheric temperature changes of ±2 °C resulted in $\delta^{18}O_{lw}$ changes of +1.21‰ and −1.26‰ (Supplemental Fig. 6). The same test produced theoretical equilibrium summer $\delta^{18}O_{cal}$ shifts of +0.78‰ and −0.68‰ VPDB (Fig. 5). Notably, the amplitude of modeled summer $\delta^{18}O_{cal}$ values is similar to the range of measured Cheeseman Lake $\delta^{18}O_{cal}$ values. Precipitation seasonality tests focus on changes in the winter (herein defined as the period between October and March) and summer (April to September). Winter season precipitation changes of ±20% resulted in $\delta^{18}O_{lw}$ shifts of −0.12‰ and +0.17‰ (Supplemental Fig. 6). The same test produced theoretical equilibrium summer $\delta^{18}O_{cal}$ variations of −0.11‰ and +0.17‰ VPDB (Fig. 5). Summer season precipitation changes of ±20% resulted in $\delta^{18}O_{lw}$ shifts of +0.12‰ and −0.08‰ (Supplemental Fig. 6) and theoretical equilibrium summer $\delta^{18}O_{cal}$ anomalies of +0.08‰ and −0.05‰ VPDB (Fig. 5).

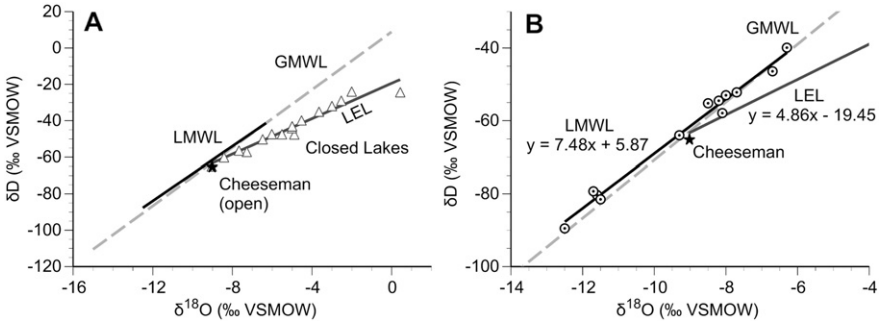

Fig. 3. (a) Surface water $\delta^{18}O$-δD data (VSMOW) from Cheeseman Lake (black star) and regional lakes (open triangles) collected in August 2012 (Supplemental Table 1). The Cheeseman Lake surface water sample plots along the Local Meteoric Water Line (LMWL, black line) developed with a linear, best-fit line from monthly average precipitation $\delta^{18}O$ and δD from the Bay d'Espoir Canadian Network of Isotopes in Precipitation (CNIP) station in south-central Newfoundland (Table 2). The LMWL parallels the Global Meteoric Water Line (GMWL, dashed grey line). Regional lakes sensitive to evaporation plot along a Local Evaporation Line (LEL, solid grey line) that is oblique to the LMWL and GMWL. (b) Same as in (a) but with a focus on the intersection of the LMWL and the LEL and with monthly precipitation isotope values (dotted circles).

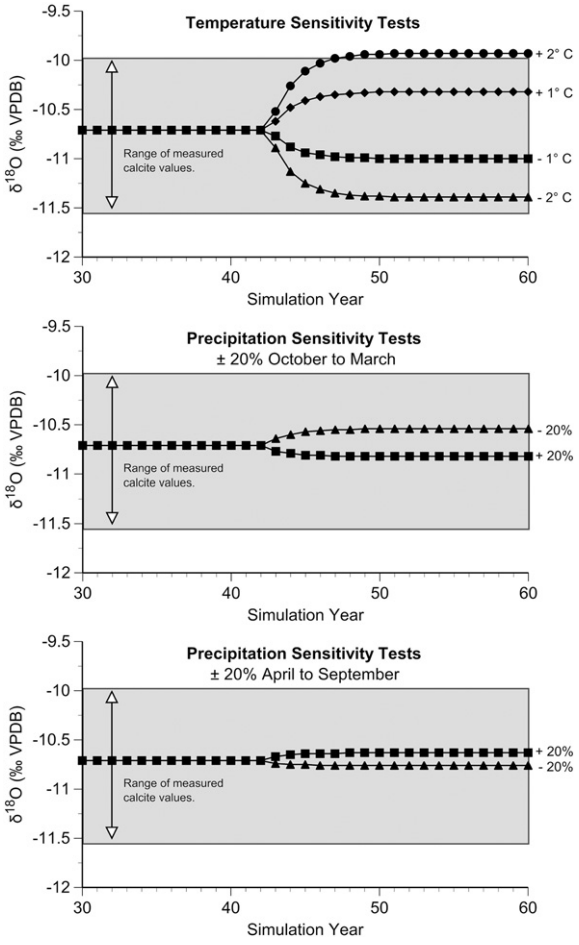

Fig. 5. Simulated summer (June–August) calcite $\delta^{18}O$ (‰ VPDB) values from annual temperature sensitivity tests of ±1 °C and ±2 °C (top panel) and for changes in winter-season (± 20% October to March, middle panel) and summer-season (± 20% April to September, middle panel) precipitation amounts (bottom panel). The grey boxes depict the range of measured calcite $\delta^{18}O$ values from the Cheeseman Lake sediment record.

5. Discussion

5.1. Interpretation of calcite oxygen isotopes

The oxygen isotope composition of lacustrine authigenic calcite ($\delta^{18}O_{cal}$) is a function of the isotopic composition of lake water ($\delta^{18}O_{lw}$) and the temperature of calcite precipitation (Gat, 1995; Kim and O'Neil, 1997). In open-basin lakes with short water residence times (e.g. Cheeseman Lake) the $\delta^{18}O_{lw}$ is principally controlled by the oxygen isotopic composition of precipitation and inflow from the catchment and groundwater ($\delta^{18}O_{ppt}$) (Gat, 1995). At mid to high-latitude sites, the $\delta^{18}O_{ppt}$ is systematically related to atmospheric temperature (Dansgaard, 1964), with a global relationship wherein a ~ 0.6‰ increase in $\delta^{18}O_{ppt}$ occurs per 1 °C increase in air temperature (and vice versa) (Rozanski et al., 1992). Seasonal variations in temperature coincide with concomitant changes in $\delta^{18}O_{ppt}$ for Newfoundland (Table 2), such that cold-season $\delta^{18}O_{ppt}$ values are substantially more negative in comparison with warm-season values (Rozanski et al., 1992). Changes in precipitation seasonality are therefore a potentially strong control on lake water $\delta^{18}O$ variability, even though modern precipitation is generally distributed equally over the year (Supplemental Fig. 2). $\delta^{18}O_{ppt}$ is also controlled by the rain-out history of an air mass, through the latitude, altitude, and continental effects that produce a progressive depletion of $\delta^{18}O_{ppt}$ via Rayleigh distillation (Dansgaard, 1964).

Cheeseman Lake surface water $\delta^{18}O_{lw}$ plots on the LMWL (Fig. 3), suggesting negligible evaporative modification and that water loss is primarily through surficial outflow and groundwater outseepage (non-fractionating pathways). These $\delta^{18}O_{lw}$ measurements combined with a lack of covariance between calcite $\delta^{18}O$ and $\delta^{13}C$ values ($r^2 = 0.07$; not shown) (Li and Ku, 1997) and physical observations indicating an open-basin hydrology suggest that Cheeseman Lake $\delta^{18}O_{cal}$ values are primarily controlled by the oxygen isotope composition of precipitation ($\delta^{18}O_{ppt}$), which itself is strongly influenced by atmospheric temperature. In the past, authigenic calcite likely precipitated at Cheeseman Lake during the summer months through photosynthetically mediated increases in pH resulting from algal utilization of dissolved CO_2, which produced greater HCO_3– and CO_3– concentrations and thereby induced carbonate mineral precipitation (Kelts and Hsu, 1978). This interpretation is supported by on-site observations in August 2012 and a review of Landsat satellite imagery that indicate 'whiting' events of carbonate precipitation in the summer months within lakes in west-central Newfoundland. Accordingly, Cheeseman Lake $\delta^{18}O_{cal}$ should reflect the $\delta^{18}O_{lw}$ and the summer lake water temperature at the time of calcification (Kim and O'Neil, 1997).

Model sensitivity test results provide support for the interpretation that atmospheric temperature is a strong influence on Cheeseman Lake $\delta^{18}O_{lw}$ and $\delta^{18}O_{cal}$ and that variations in the seasonality of precipitation are relatively less influential. For example, temperature changes of ±2 °C produce theoretical summer $\delta^{18}O_{cal}$ values with a range similar to that of measured down-core $\delta^{18}O_{cal}$ values (Fig. 5); whereas winter and summer season precipitation changes of ±20% yield theoretical summer $\delta^{18}O_{cal}$ anomalies that are too small to explain the range of measured $\delta^{18}O_{cal}$ values (Fig. 5). Consequently, changes in the seasonality of precipitation, while still important, must be considered a secondary control on variations in $\delta^{18}O_{ppt}$ and $\delta^{18}O_{cal}$.

Other factors affecting the $\delta^{18}O_{ppt}$ over the Holocene include changes in the regional precipitation source resulting from shifts in atmospheric circulation (Birks and Edwards, 2009), as well as temporal variability in the isotopic composition of ocean source water (Araguás-Araguás et al., 2000). The modern source of precipitation for Newfoundland is predominantly from the west in the Gulf of St. Lawrence and from the south in the western Atlantic Ocean, originating via cyclonic or frontal activity (Ullah, 1992; Milrad et al., 2010). The influence of Arctic or Pacific Ocean derived-precipitation to Newfoundland is presumably negligible, at least on centennial to millennial time scales, given the small range in Cheeseman Lake $\delta^{18}O_{cal}$ values (~ 1.5‰) over the middle to late Holocene. During the early Holocene, however, the $\delta^{18}O$ composition of North Atlantic surface waters varied substantially as a result of Laurentide and Greenland Ice Sheet deglaciation and meltwater flux to both the Labrador Sea and western Atlantic Ocean (Andrews et al., 1999; Keigwin et al., 2005; Hoffman et al., 2012). Furthermore, the presence of the Laurentide Ice Sheet (LIS) in eastern North America during the early Holocene influenced atmospheric circulation patterns in Newfoundland (Bartlein et al., 2014), which likely had a strong impact on $\delta^{18}O_{ppt}$. Climate model simulations show a weak anticyclone centered over the southern edge of the LIS at 9000 ^{14}C yr BP (10,200 cal yr BP) (Bartlein et al., 2014), which resulted in northerly winds and the delivery of cold, dry air in downstream regions including Newfoundland. Disintegration of the LIS by 6000 ^{14}C yr BP (6800 cal yr BP) lead to the establishment of modern westerly winds across North America and atmospheric circulation patterns similar to those of present day. We therefore hypothesize that changes in Earth's surface boundary conditions produced variations in Newfoundland precipitation regimes, which are recorded by $\delta^{18}O$ values in Cheeseman Lake sediment.

5.2. Newfoundland regional comparison

The Nordan's Pond Bog $\delta^{18}O_{ppt}$ reconstruction (Fig. 6), based on isotope analysis of sedimentary cellulose, is the only other available isotope record of precipitation changes from Newfoundland (Daley et al., 2009). The major difference between the two records is the much larger

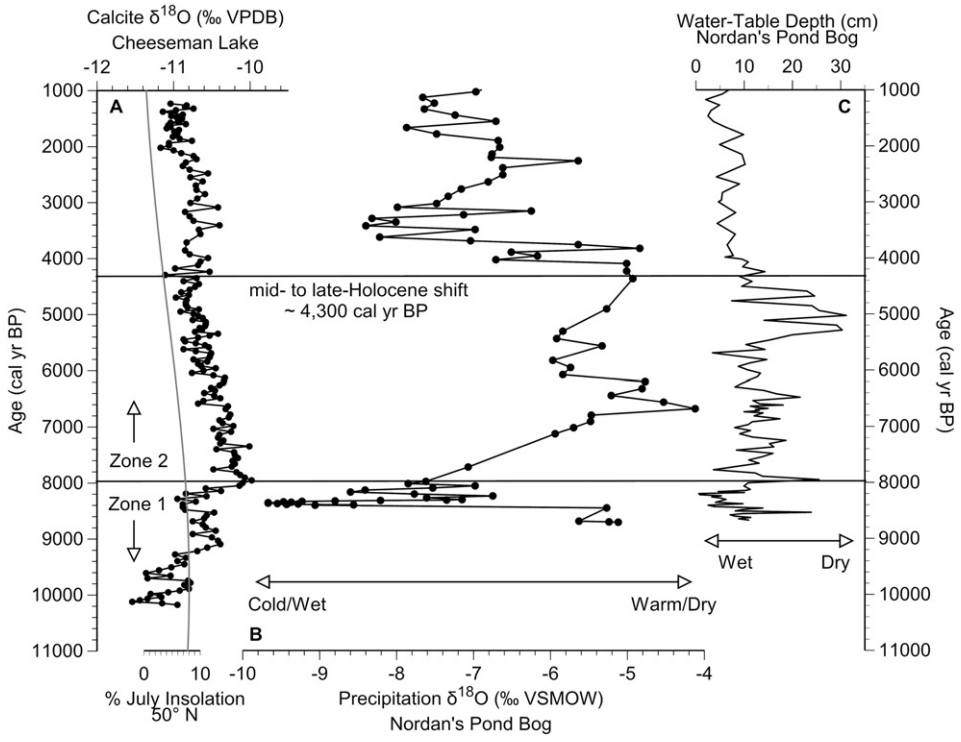

Fig. 6. Regional comparison of hydroclimate reconstructions from Newfoundland including (a) Cheeseman Lake carbonate $\delta^{18}O$ (‰ VPDB) and the % July insolation difference compared to modern (Laskar et al., 2004), (b) Nordan's Pond Bog $\delta^{18}O$ (‰ VSMOW) (Daley et al., 2009), and (c) Nordan's Pond Bog testate-amoeba based water-table depth reconstruction (Hughes et al., 2006; Amesbury et al., 2013). The Zone 1 and Zone 2 transition in the Cheeseman Lake record occurs at ~8000 cal yr BP and a middle to late-Holocene climate shift occurs at ~4300 cal yr BP.

range (of 5.5‰) in $\delta^{18}O$ values from Nordan's Pond Bog relative to that of Cheeseman Lake (1.5‰). Given the relatively short distance between the sites (~ 300 km), we assert that spatial variations in $\delta^{18}O_{ppt}$, as observed in other paleorecords (Edwards et al., 1996; Kirby et al., 2002), cannot explain this difference in the magnitude of $\delta^{18}O$ variations, and that differences in lake/bog hydrology, sampling resolution, and isotopic fractionations specific to each proxy type are the likely reason for the inconsistency. Regarding lake/bog hydrology, we suggest that Nordan's Pond Bog is strongly influenced by evaporation and water balance variations, given its relatively large surface area to volume ratio, and exhibits stronger hydrologic and isotopic responses to variations in precipitation-evaporation (*P*-E) balance than does Cheeseman Lake. This idea is supported by the isotopic composition of bog waters ($n = 8$) collected in July of 2004, which plot along and therefore define the local evaporation line (Daley et al., 2009). The $\delta^{18}O$ record from Nordan's Pond Bog primarily reflects past changes in *P*-E or water balance, with relatively positive $\delta^{18}O_{ppt}$ values resulting from some combination of warmer temperatures and enhanced evaporation, reduced precipitation, and/or a shift in precipitation from the cold to the warm season (and vice versa). Cheeseman Lake, in contrast, is an open-basin lake that overflows through a surficial outlet and has a much lower surface area to volume ratio making it less sensitive to evaporative modification. These interpretations are further supported by a testate-amoeba based water-table depth reconstruction by Hughes et al. (2006) and Amesbury et al. (2013) (Fig. 6), which shows substantial shifts in water balance coincident with $\delta^{18}O_{ppt}$ variations. Differences in proxy sampling resolution also help to explain disparity between the two records. For instance, the Cheeseman Lake proxy resolution is ~50 years/sample and therefore captures multi-decadal to sub-century scale variations in $\delta^{18}O_{ppt}$ and atmospheric temperature. Although discontinuously sampled, the Nordan's Pond Bog $\delta^{18}O_{ppt}$ reconstruction has a higher resolution of ~10 years/sample, which can potentially resolve larger magnitude decadal scale anomalies. With respect to the proxy sensitivity, we assert that the temperature dependent fractionation of the water-calcite transformation for Cheeseman Lake of −0.24‰/°C (Craig, 1965) must be accounted for when comparing the temperature-$\delta^{18}O$ anomalies between the records. Dissimilarly, at Nordan's Pond Bog the isotope values of cellulose are affected by water-cell fractionation processes that are accounted for through the application of a constant correction factor for data spanning the past 8900 cal yr BP (Daley et al., 2009).

Using the globally defined temperature-$\delta^{18}O_{ppt}$ relationship of 0.6‰/°C and accounting for the temperature dependence of the water-calcite transformation, the range in observed $\delta^{18}O$ values corresponds with a 9.2 °C and 4.2 °C temperature range for Nordan's Pond Bog and Cheeseman Lake, respectively. This substantial difference of 5 °C cannot be explained by climatic processes and must be a product of disparity in the information recorded by the two isotopic proxies. As a result, we interpret the large differences observed between the records and specifically across the 8200 cal yr BP event to reflect water balance variations and evaporative modification at Nordan's Pond Bog, and to a lesser extent, proxy resolution differences between the records and the temperature dependence of carbonate precipitation at Cheeseman Lake. This result has implications for climate model simulations of the 8200 cal yr BP abrupt climate event (Daley et al., 2011; Tindall and Valdes, 2011), which suggest that greater negative $\delta^{18}O_{ppt}$ excursions are experienced proximal to the Labrador Sea in the region of North Atlantic Deep Water formation shutdown.

The Cheeseman Lake $\delta^{18}O_{cal}$ record and Nordan's Pond Bog $\delta^{18}O_{ppt}$ reconstruction are substantially different, yet there are a few similarities (Fig. 6). For instance, both records exhibit anomalous shifts to more negative $\delta^{18}O$ values associated with the 8200 cal yr BP abrupt climate change event during the early Holocene (Alley et al., 1997; Barber et al., 1999). The transition to more negative values at Cheeseman Lake occurs at ~8500 cal yr BP and is characterized by a − 0.38‰ (VPDB) excursion. At Nordan's Pond Bog, the transition begins at ~8400 cal yr BP and is characterized by a − 3.79‰ (VSMOW) excursion. Using the globally defined temperature-$\delta^{18}O_{ppt}$ relationship of 0.6‰/°C and accounting

for the temperature dependence of the water-calcite transformation of −0.24‰/°C (Craig, 1965), these changes correspond with a 1.1 °C cooling at Cheeseman Lake and a 6.3 °C cooling at Nordan's Pond Bog. Notably, the application of modern temperature-$\delta^{18}O_{ppt}$ relationships to the early Holocene is only marginally informative given this relationship was likely different then due to differences in atmospheric circulation resulting from the presence of the LIS (Bartlein et al., 2014).

After the 8200 cal yr BP event, Cheeseman Lake $\delta^{18}O_{cal}$ values increase, reaching the most positive values (−10.0‰) during the entire record at 8000 cal yr BP (Fig. 6). Thereafter, Cheeseman Lake $\delta^{18}O_{cal}$ values decrease and eventually attain minimum values (−11.1‰) around ~4300 cal yr BP. We interpret these variations to represent warm conditions and/or enhanced warm-season precipitation immediately after 8000 cal yr BP and gradual cooling thereafter. In contrast, Nordan's Pond Bog $\delta^{18}O_{ppt}$ values increase after 8200 cal yr BP and are relatively high (~ −4 to −6‰) between 6800 and 3900 cal yr BP (Fig. 6). We interpret this discrepancy to indicate increased evaporation at Nordan's Pond Bog, resulting in more positive $\delta^{18}O_{ppt}$ values, consistent with drier conditions during this time (Amesbury et al., 2013). After 3900 cal yr BP, $\delta^{18}O_{ppt}$ values at Nordan's Pond Bog decrease abruptly by ~4‰ and remain relatively low (between ~ −6 to −8‰) for the remainder of the Holocene (Fig. 6). This transition likely reflects the onset of wetter conditions and reduced evaporation of bog waters, consistent with the inferred higher and more stable water-table depth at Nordan's Pond Bog after ~4000 cal yr BP (Fig. 6) (Hughes et al., 2006; Amesbury et al., 2013). Concurrently, Cheeseman Lake $\delta^{18}O_{cal}$ briefly returns to relatively higher values of −10.4‰ between ~3400 to ~3000 cal yr BP, indicating slightly warmer conditions at this time, and exhibits a slight trend towards more negative and generally stable values thereafter.

5.3. North Atlantic comparison: The early Holocene (10,200 to 8000 cal yr BP)

The 1.5‰ increase in Cheeseman Lake $\delta^{18}O_{cal}$ values between 10,200 and 8000 cal yr BP (Fig. 7) implies a 4.2 °C temperature increase, assuming the shift in $\delta^{18}O$ was entirely driven by atmospheric temperature changes. A similar trend is found at this time in both the Dye-3 and NGRIP Greenland ice core $\delta^{18}O$ records (Fig. 7), which has been interpreted to reflect rising temperatures during the final stages of deglaciation (Vinther et al., 2009). It is unlikely, however, that the increase in Cheeseman Lake $\delta^{18}O_{cal}$ reflects temperature changes alone, because this period coincides with the disintegration and final retreat of the Laurentide Ice Sheet (Dyke and Prest, 1987), as well as the attendant shifts in atmospheric circulation, and enhanced glacial meltwater flux to the Labrador Sea and western Atlantic Ocean. Along these lines, gradually decreasing planktonic foraminiferal (*N. pachyderma sinistral*) $\delta^{18}O$ values recorded south of Newfoundland at the Laurentian Fan (Fig. 7) reflect changes in the $\delta^{18}O$ of the surface ocean from ice sheet retreat (Keigwin et al., 2005), which likely influenced $\delta^{18}O_{ppt}$ at Cheeseman Lake by changing the isotopic composition of the source of precipitation delivered to Newfoundland. The increase in Cheeseman Lake $\delta^{18}O_{cal}$ is interrupted by abrupt negative excursions at ~9700 and ~8500 cal yr BP. The ~9700 cal yr BP feature occurs too early to be linked with the ~9300 cal yr BP climate change event identified by Yu et al. (2010), suggesting that the Cheeseman Lake $\delta^{18}O_{cal}$ record is either too coarsely resolved in time to detect this rather short-lived event, or the event did not substantially influence climate in western Newfoundland. The ~9700 cal yr BP excursion at Cheeseman Lake does, however, coincide with a shift towards colder sea surface temperatures (SSTs) and decreasing surface ocean $\delta^{18}O$ ($\delta^{18}O_{sw}$) at Cartwright Saddle in the western Labrador Sea (Fig. 7), which Hoffman et al. (2012) interpret to reflect enhanced meltwater flux and renewed Laurentide Ice Sheet retreat. Similar to the 9700 cal yr BP event, the Cheeseman Lake $\delta^{18}O_{cal}$ excursion at ~8500 cal yr BP also coincides with a shift to colder SSTs at Cartwright Saddle (Hoffman et al., 2012) associated with the final drainage of Glacial Lake Agassiz (Barber et al., 1999), indicating a synchronous response between the regional ocean-atmosphere system at this time. Similar phasing is found in the Nordan's Pond Bog $\delta^{18}O_{ppt}$, wherein the primary shift begins at ~8400 cal yr BP (Daley et al., 2009, 2011). Through this interval, the Greenland ice cored $\delta^{18}O$ data is not consistent with the Cheeseman Lake $\delta^{18}O_{cal}$ record, shifting to more negative values almost ~300 years later than at Cheeseman Lake (Fig. 7), which

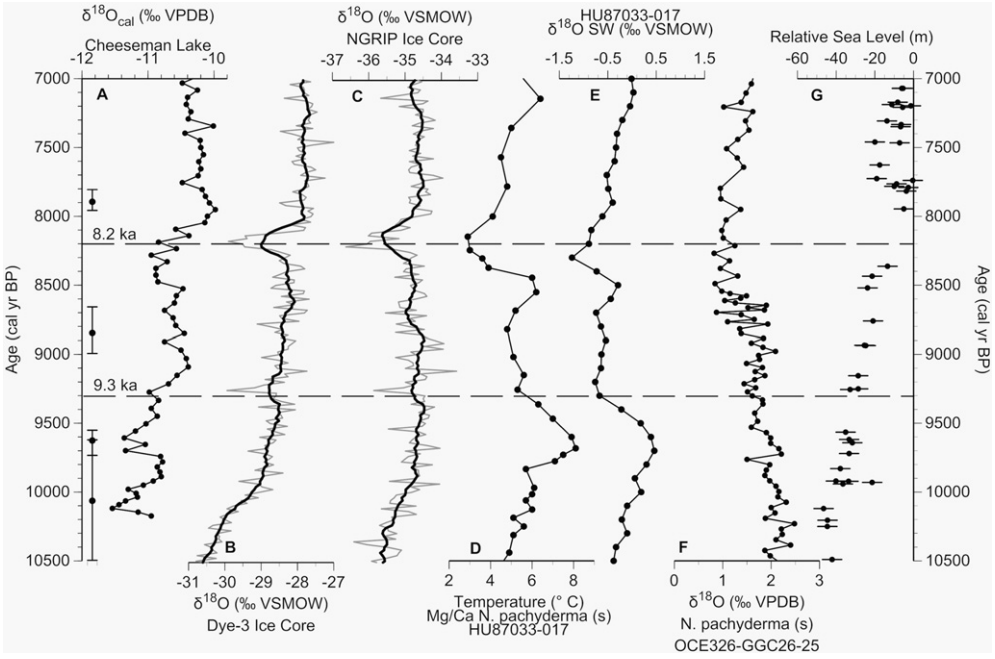

Fig. 7. Comparison of early Holocene climate records from the North Atlantic region, including (a) Cheeseman Lake carbonate $\delta^{18}O$ with calibrated median radiocarbon ages and the 95% error bounds on the left. (b) Dye-3 ice core $\delta^{18}O$ (grey line) and 200-yr moving average (black line) (Dansgaard et al., 1985). (c) NGRIP ice core $\delta^{18}O$ (grey line) and 200-yr moving average (black line) (NGRIP, 2004). (d) Mg/Ca inferred calcification temperature of the planktonic foraminifer *N. pachyderma sinistral* from marine core HU87033–017 from the Cartwright Saddle in the Labrador Sea (Hoffman et al., 2012). (e) $\delta^{18}O$ of sea water from marine core HU87033–017 (Hoffman et al., 2012). (f) *N. pachyderma sinistral* $\delta^{18}O$ from marine core OCE326-GGC26–25 from the Laurentian Fan south of Newfoundland (Keigwin et al., 2005). (g) Relative eustatic sea level anomalies (Clark et al., 2009 and references therein).

likely reflects local climate responses or alternatively chronological uncertainty. The Cheeseman Lake sediment, for example, could be as much as ~200 years younger at this time than is suggested by the median ages of the age model and still fall within the 2sigma uncertainty range.

After ~8280 cal yr BP, Cheeseman Lake $\delta^{18}O_{cal}$ values increase from −10.9‰ to maximum values of −10.0‰ by 8000 cal yr BP (Fig. 7). Converting this 0.9‰ increase in $\delta^{18}O_{cal}$ values yields a temperature increase of 2.5 °C spanning the ~350 year period. However, $\delta^{18}O_{ppt}$ across Newfoundland at this time was likely controlled by a number of other factors including changes in P-E (Amesbury et al., 2013), the seasonality of precipitation, surface ocean $\delta^{18}O$ (Keigwin et al., 2005; Hoffman et al., 2012), and atmospheric circulation (Edwards et al., 1996; Kirby et al., 2002). Thus, we conclude that the post 8200 cal yr BP transition to the most positive $\delta^{18}O_{cal}$ values of the Holocene reflects some combination of warmer atmospheric temperatures, a shift back to greater warm-season precipitation, and potentially wetter conditions.

5.4. North Atlantic comparison: The middle to late Holocene (8000 to 1200 cal yr BP)

The Cheeseman Lake $\delta^{18}O_{cal}$ record suggests that immediately after 8000 cal yr BP the warmest conditions of the Holocene occurred (Fig. 8). This result is consistent with a synthesis of temperature reconstructions from the western North Atlantic region, which shows the warmest Holocene temperatures in eastern Canada between 8000 and 6000 cal yr BP (Kaplan and Wolfe, 2006). Additional evidence for this pattern is provided by Greenland ice core $\delta^{18}O$ records (Fig. 8), which indicate the warmest temperatures of the Holocene at ~7900 cal yr BP (Vinther et al., 2009). This period of warming lags the early Holocene 50°N summer insolation maxima by 1000 to 3000 years in the western Atlantic Ocean region. The lag in peak temperatures with respect to insolation forcing is attributed to the close proximity of the residual Laurentide Ice Sheet and the cooling effect it imparted to Newfoundland prior to ice sheet disintegration (Bartlein et al., 2014).

Cheeseman Lake $\delta^{18}O_{cal}$ gradually decreased between 8000 and 4300 cal yr BP (Fig. 8), consistent with the monotonic decline in high-latitude Northern Hemisphere summer insolation (Laskar et al., 2004). The 1.1‰ decrease in $\delta^{18}O_{cal}$ values over this time period represents a 3.1 °C cooling, assuming temperature is the only factor influencing $\delta^{18}O_{ppt}$ at Cheeseman Lake and using the modern temperature-$\delta^{18}O_{ppt}$ relationship of 0.6‰/°C. A similar response occurred in the Greenland ice core $\delta^{18}O$ records (Fig. 8) and ice-core inferred temperatures, which translates to a 2.7 °C cooling from 8000 to 4300 cal yr BP (Vinther et al., 2009). Evidence for cooling at this time is also found in proximal oceanographic records from the Laurentian Fan south of Newfoundland, where alkenone-derived SSTs decrease from 8000 cal yr BP to the present (Keigwin et al., 2005; Sachs, 2007). Keigwin et al. (2005) suggest that the long term decrease in SSTs (and increase in foraminiferal $\delta^{18}O$ values) is driven by decreasing seasonality of Northern Hemisphere insolation forced by gradually decreasing summer and increasing winter insolation through the Holocene (Fig. 8) (Laskar et al., 2004). More specifically, Sachs (2007) attributed the cooling of continental slope waters at the Laurentian Fan and along the eastern seaboard of North America to declining insolation, increasing convection in the Labrador Sea, and an equatorward shift of the Gulf Stream that would have affected the source and $\delta^{18}O$ values of precipitation delivered to Newfoundland. Thus, the concurrent shifts in Cheeseman Lake $\delta^{18}O_{cal}$ and the inferred cooling of Newfoundland support the notion of a coupled ocean-atmosphere response to insolation forcing at millennial time scales, at least between 8000 and 4300 cal yr BP.

The spatial pattern in reco nstructed SSTs from the Laurentian Fan and across the Atlantic Ocean during the Holocene implicates a possible role of the North Atlantic Oscillation (NAO) in driving the regional decline in temperatures. A positive phase of the NAO (NAO+) promotes colder conditions in Newfoundland (Hurrell and Deser, 2009), and vice versa during the negative NAO phase (NAO-). Accordingly, NAO+ and cooler winter conditions in Newfoundland should result in more negative $\delta^{18}O_{ppt}$ and $\delta^{18}O_{cal}$ at Cheeseman Lake. Based on the Holocene pattern of Atlantic-wide SSTs, Sachs (2007) suggest a transition from NAO- in the early Holocene to NAO+ by the late Holocene. This interpretation is supported by excursions in the Transpolar Drift Stream evinced from driftwood in the Canadian Arctic Archipelago, which shows early Holocene NAO- or NAO neutral conditions and NAO+ during the late Holocene (Tremblay et al., 1997). If we assume the spatial

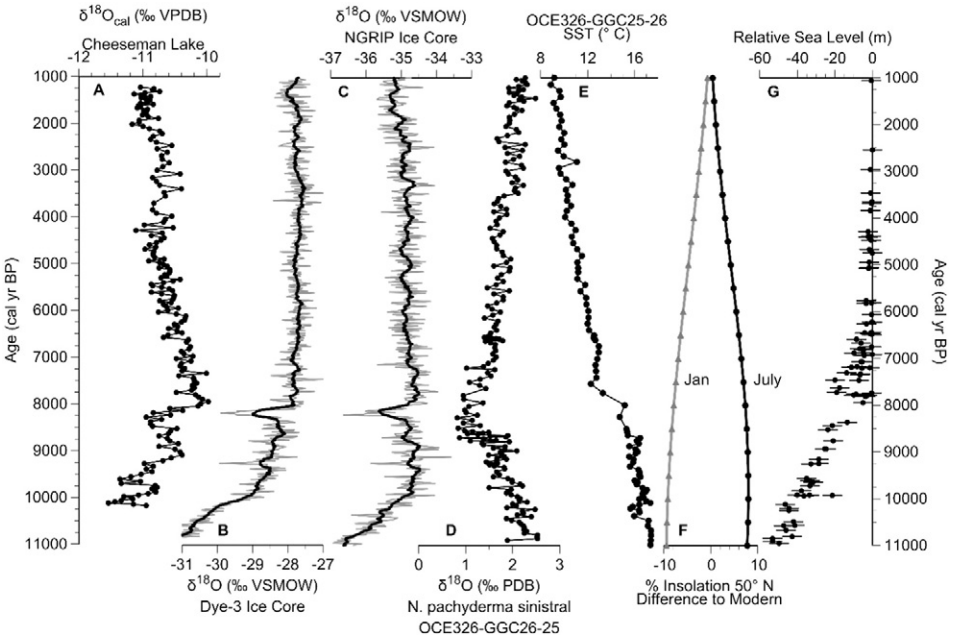

Fig. 8. Comparison of Holocene climate records from the North Atlantic region including (a) Cheeseman Lake carbonate $\delta^{18}O$. (b) Dye-3 ice core $\delta^{18}O$ (grey line) and 200-yr moving average (black line) (Dansgaard et al., 1985). (c) NGRIP ice core $\delta^{18}O$ (grey line) and 200-yr moving average (black line) (NGRIP, 2004). (d) N. pachyderma sinistral $\delta^{18}O$ (‰ VPDB) from marine core OCE326-GGC26–25 (Keigwin et al., 2005). (e) Alkenone derived sea surface temperatures (SST) from marine core OCE326-GGC26–25 (Keigwin et al., 2005; Sachs, 2007). (f) Percent insolation difference from modern for 50° North (Laskar et al., 2004). (g) Relative eustatic sea level anomalies (Clark et al., 2009 and references therein).

pattern of NAO-type conditions observed during the 20th century (Supplemental Fig. 3) persisted throughout the Holocene, such a pattern identified by Sachs (2007) would have promoted warmer temperatures during the mid-Holocene and a colder climate during the late-Holocene. The positive $\delta^{18}O_{cal}$ values at Cheeseman Lake, inferred to have resulted from relatively warm temperatures between 8000 and 4300 cal yr BP, provide evidence to support the hypothesis of Sachs (2007). However, other paleoclimate synthesis studies show the opposite, that the early Holocene was typified by a positive NAO phase that transitioned to NAO- during the late-Holocene (Rimbu et al., 2004). This discrepancy highlights the need for additional paleo reconstructions of NAO-like circulation variability during the Holocene.

After 4300 cal yr BP, the pattern of decreasing Cheeseman Lake $\delta^{18}O_{cal}$ is interrupted by a minor positive excursion (Fig. 8), discordant with the continual decline in high-latitude Northern Hemisphere summer insolation (Laskar et al., 2004). This return to slightly more positive and relatively stable $\delta^{18}O_{cal}$ values from ~4000 and ~2500 cal yr BP could in part reflect marginally warmer temperatures and/or, secondarily, a decrease in cold-season or increase in warm-season precipitation (Fig. 5). Alternatively, the $\delta^{18}O_{cal}$ trend could be in part controlled by increased evaporative modification of lake water. However, this transition coincides with a shift to wetter conditions by 4000 cal yr BP and a 3.9‰ negative shift in $\delta^{18}O$ values at 3900 cal yr BP at Nordan's Pond Bog in eastern Newfoundland (Fig. 6) (Hughes et al., 2006; Daley et al., 2009; Amesbury et al., 2013). Palynological evidence also provides support for major climate change across Newfoundland, with wetter conditions inferred from an increase in *Alnus* shrubs and corresponding decrease in *Pinus* taxa after 4000 cal yr BP (MacPherson, 1995). Collectively, the regional proxy evidence suggests that a reorganization of atmospheric circulation occurred at this time across Newfoundland and the greater north Atlantic region. After ~2500 cal yr BP, Cheeseman $\delta^{18}O_{cal}$ values decline to the most depleted values of the late Holocene, indicating the return of cooler conditions.

The middle to late-Holocene transition in Cheeseman Lake $\delta^{18}O_{cal}$, proxy evidence from Nordan's Pond Bog, and palynological evidence from across Newfoundland coincides with widespread regional and global evidence for a climatic shift between ~5000 and ~4000 cal yr BP (Booth et al., 2005; Liu et al., 2014; Roland et al., 2014). For instance, Booth et al. (2005) synthesized mid-continent North American hydroclimate records and reported evidence for a severe drought between 4300 and 4100 cal yr BP in low to middle latitude sites, while many higher latitude locations experienced a shift to wetter conditions (Booth et al., 2005). Liu et al. (2014) analyzed oxygen isotope records from western and eastern North America and suggest that a negative mean state of the Pacific-North American (PNA) pattern persisted during the middle Holocene followed by a transition around 4000 cal yr BP to a more positive PNA-like climate. The PNA influences North American weather patterns through its effect on the strength and location of the East Asian jet stream, which is the primary driver of atmospheric circulation (zonal vs. meridional flow) over the continent, especially during the winter. Evidence from at mospheric model simulations indicate that PNA+ conditions result in positive $\delta^{18}O_{ppt}$ anomalies in Atlantic Canada during the winter and on an annual basis (Liu et al., 2014), which likely reflects the combined influence of warmer temperatures and greater inputs of warm season precipitation. Variations in the PNA are further driven by internal ocean-atmosphere variability, in particular the El Niño Southern Oscillation and Pacific Decadal Oscillation, which in turn respond to external forcing over a range of time scales. This shift from a negative to positive PNA mean state likely produced a transition from zonal to greater meridional atmospheric circulation through the middle to late Holocene, which in turn influenced the winter position of the polar front, atmospheric temperature, and the $\delta^{18}O_{ppt}$ across North America. Additional $\delta^{18}O_{ppt}$ reconstructions from the mid-Atlantic and Great Lakes region (Edwards et al., 1996; Yu et al., 1997; Kirby et al., 2002) support this hypothesis. The Cheeseman lake oxygen isotope record, as well as other paleoclimate data from Newfoundland (MacPherson, 1995; Hughes et al., 2006; Daley et al., 2009; Amesbury et al., 2013), provide an important western Atlantic geographic perspective and thereby reinforce the idea that a hemisphere wide shift in ocean-atmosphere circulation drove a large-scale reorganization of North American climate during the middle to late-Holocene transition (between ~5000 to ~4000 cal yr BP).

6. Conclusions

Lake hydrologic and isotope mass balance model simulations and measurements of regional water isotope values indicate that the Cheeseman Lake $\delta^{18}O_{cal}$ record provides insight into the Holocene evolution of $\delta^{18}O_{ppt}$ and temperature in northeastern North America. A general trend of increasing and more positive $\delta^{18}O_{cal}$ values between 10,200 and 8000 cal yr BP is interpreted to reflect warming temperatures, the waning influence of the Laurentide Ice Sheet on atmospheric circulation and rapidly changing surface ocean $\delta^{18}O$ from the input of glacial meltwater to the western North Atlantic Ocean. This increasing trend is interrupted by abrupt, negative $\delta^{18}O_{cal}$ anomalies at 9700 cal yr BP, associated with a transition to colder sea surface temperatures (SST's) in the Labrador Sea and renewed Laurentide Ice Sheet retreat (Hoffman et al., 2012), and at 8500 cal yr BP that coincides with a well-established cooling event in the circum-North Atlantic region (Alley et al., 1997). After 8000 cal yr BP, $\delta^{18}O_{cal}$ values gradually decrease to more negative values until 4300 cal yr BP, indicating a long term cooling trend, consistent with declining Boreal summer insolation and cooling SSTs in the western North Atlantic Ocean. $\delta^{18}O_{cal}$ values return to slightly more positive values after 4300 to 2500 cal yr BP and thereafter decline to the most depleted values of the late Holocene. The middle to late-Holocene transition at around 4300 cal yr BP corresponds with a shift to wetter conditions in Newfoundland evinced from other paleo-proxy records. The discordance between Cheeseman Lake $\delta^{18}O_{cal}$ values and declining insolation could in part reflect warmer temperatures and/or changes in the seasonality of precipitation at this time. In light of evidence from other paleo-records in Newfoundland, the shift around 4300 cal yr BP likely resulted from a change in atmospheric circulation associated with the transition to a positive mean state phase of the Pacific-North American pattern. Proxy evidence from Cheeseman Lake provides a terrestrial, western Atlantic geographic perspective that supports the idea of substantial climatic change on a hemispheric scale during the Holocene overall and particularly during middle to late-Holocene transition.

The Cheeseman Lake data presented here will be archived at the National Climatic Data Center (https://www.ncdc.noaa.gov/data-access/paleoclimatology-data/datasets/lake).

Acknowledgements

Funding for this project was provided by startup funds from Abbott. Finkenbinder recognizes support from the Mellon Predoctoral Fellowship from the University of Pittsburgh during the writing of this manuscript. We would like to thank Jordan and Graham Abbott for their help with fieldwork; John Southon and Chanda Bertrand at the Keck Carbon Cycle Accelerator Mass Spectrometry Laboratory at the University of California, Irvine for assistance in preparing graphite targets and radiocarbon measurement; Thomas Edwards at the University of Waterloo for providing the Bay d'Espoir precipitation isotope data; Matthew Amesbury at the University of Exeter for providing the Nordan's Pond Bog water-table depth reconstruction data; Kaitlyn Clark for assistance with the XRD and SEM measurements; Rob McDermott and Justin Coughlin for assistance with carbonate preparation; and Aubrey Hillman and David Pompeani for helpful discussion on the research. We thank Matthew Amesbury and an anonymous reviewer for comments and suggestions that greatly improved the manuscript.

Appendix A. Supplementary data

Supplementary data to this article can be found online at http://dx.doi.org/10.1016/j.gloplacha.2016.06.014.

References

Alley, R.B., Mayewski, P.A., Sowers, T., Stuiver, M., Taylor, K.C., Clark, P.U., 1997. Holocene climatic instability: a prominent, widespread event 8200 years ago. Geology 25, 483–486.

Amesbury, M.J., Mallon, G., Charman, D.J., Hughes, P.D.M., Booth, R.K., Daley, T.J., Garneau, M., 2013. Statistical testing of a new testate amoeba-based transfer function for water-table depth reconstruction on ombrotrophic peatlands in north-eastern Canada and Maine, United States. J. Quat. Sci. 28, 27–39.

Andrews, J.T., Keigwin, L., Hall, F., Jennings, A.E., 1999. Abrupt deglaciation events and holocene palaeoceanography from high-resolution cores, cartwright saddle, Labrador shelf, Canada. J. Quat. Sci. 14, 383–397.

Araguás-Araguás, L., Froehlich, K., Rozanski, K., 2000. Deuterium and oxygen-18 isotope composition of precipitation and atmospheric moisture. Hydrol. Process. 14, 1341–1355.

Bale, R.J., Robertson, I., Leavitt, S.W., Loader, N.J., Harlan, T.P., Gagen, M., Young, G.H.F., Csank, A.Z., Froyd, C.A., McCarroll, D., 2010. Temporal stability in bristlecone pine tree-ring stable oxygen isotope chronologies over the last two centuries. The Holocene 20, 3–6.

Banfield, C.E., Jacobs, J.D., 1998. Regional patterns of temperature and precipitation for Newfoundland and Labrador during the past century. Can. Geogr. 42, 354–364.

Barber, D.C., Dyke, A., Hillaire-Marcel, C., Jennings, A.E., Andrews, J.T., Kerwin, M.W., Bilodeau, G., McNeely, R., Southon, J., Morehead, M.D., Gagnon, J.M., 1999. Forcing of the cold event of 8200 years ago by catastrophic drainage of Laurentide lakes. Nature 400, 344–348.

Bartlein, P.J., Hostetler, S.W., Alder, J.R., 2014. Paleoclimate. In: Ohring, G. (Ed.), Climate Change in North America. Springer International Publishing, New York, NY, pp. 1–51.

Batterson, M.J., Catto, N.R., 2001. Topographically-controlled deglacial history of the Humber River basin, western Newfoundland. Géog. Phys. Quatern. 55, 213–228.

Birks, S.J., Edwards, T.W.D., 2009. Atmospheric circulation controls on precipitation isotope-climate relations in western Canada. Tellus Ser. B Chem. Phys. Meteorol. 61, 566–576.

Blaauw, M., 2010. Methods and code for 'classical' age-modelling of radiocarbon sequences. Quat. Geochronol. 5, 512–518.

Booth, R.K., Jackson, S.T., Forman, S.L., Kutzbach, J.E., Bettis, E.A., Kreig, J., Wright, D.K., 2005. A severe centennial-scale drought in mid-continental North America 4200 years ago and apparent global linkages. The Holocene 15, 321–328.

Clark, P.U., Dyke, A.S., Shakun, J.D., Carlson, A.E., Clark, J., Wohlfarth, B., Mitrovica, J.X., Hostetler, S.W., McCabe, A.M., 2009. The Last Glacial Maximum. Science 325, 710–714.

Colman-Sadd, S.P., Hayes, J.P., Knight, I., 2000. Geology of the island of Newfoundland (digital version of map 90–01 with minor revisions) Newfoundland Department of Mines and Energy. Geophys. Surv.

Compo, G.P., Whitaker, J.S., Sardeshmukh, P.D., Matsui, N., Allan, R.J., Yin, X., Gleason Jr., B.E., Vose, R.S., Rutledge, G., Bessemoulin, P., Broennimann, S., Brunet, M., Crouthamel, R.I., Grant, A.N., Groisman, P.Y., Jones, P.D., Kruk, M.C., Kruger, A.C., Marshall, G.J., Maugeri, M., Mok, H.Y., Nordli, O., Ross, T.F., Trigo, R.M., Wang, X.L., Woodruff, S.D., Worley, S.J., 2011. The Twentieth Century Reanalysis Project. Q. J. R. Meteorol. Soc. 137, 1–28.

Craig, H., 1965. The Measurement of Oxygen Isotope Palaeotemperatures. In: Tongiorgi, E. (Ed.), Stable Isotopes in Oceanographic Studies and Palaeotemperatures. Consiglio Nazionale delle Ricerche Laboratorio di Geologia Nucleare, Pisa, pp. 161–182.

Daley, T.J., Street-Perrott, F.A., Loader, N.J., Barber, K.E., Hughes, P.D.M., Fisher, E.H., Marshall, J.D., 2009. Terrestrial climate signal of the "8200 yr BP cold event" in the Labrador Sea region. Geology 37, 831–834.

Daley, T.J., Thomas, E.R., Holmes, J.A., Street-Perrott, F.A., Chapman, M.R., Tindall, J.C., Valdes, P.J., Loader, N.J., Marshall, J.D., Wolff, E.W., Hopley, P.J., Atkinson, T., Barber, K.E., Fisher, E.H., Robertson, I., Hughes, P.D.M., Roberts, C.N., 2011. The 8200 yr BP cold event in stable isotope records from the North Atlantic region. Glob. Planet. Chang. 79, 288–302.

Dansgaard, W., 1964. Stable isotopes in precipitation. Tellus 16, 436–468.

Dansgaard, W., Clausen, H.B., Gundestrup, N., Johnsen, S.J., Rygner, C., 1985. Dating and climatic interpretation of two deep Greenland ice cores. Geophys. Monogr. 33, 71–76.

Dyke, A., Prest, V.K., 1987. Late Wisconsinan and Holocene history of the Laurentide ice sheet. Géog. Phys. Quatern. 41, 237–263.

Edwards, T.W.D., Wolfe, B.B., MacDonald, G.M., 1996. Influence of changing atmospheric circulation on precipitation delta O-18-temperature relations in Canada during the Holocene. Quat. Res. 46, 211–218.

Environment Canada, 2010. In: Canada, E. (Ed.), Canadian Monthly Climate Data and 1981-2010 Normals: Deer Lake, Newfoundland.

Ersek, V., Clark, P.U., Mix, A.C., Cheng, H., Edwards, R.L., 2012. Holocene winter climate variability in mid-latitude western North America. Nat. Commun. 3, 1–8.

Gat, R.J., 1995. Stable Isotopes of Fresh and Saline Lakes. In: Lerman, A., Imboden, D.M., Gat, J.R. (Eds.), Physics and Chemistry of Lakes. Springer Berlin Heidelberg, Berlin, pp. 139–165.

Grootes, P.M., Stuiver, M., 1997. Oxygen 18/16 variability in Greenland snow and ice with 10(−3)- to 10(5)-year time resolution. J. Geophys. Res.-Oceans 102, 26455–26470.

Heiri, O., Lotter, A.F., Lemcke, G., 2001. Loss on ignition as a method for estimating organic and carbonate content in sediments: reproducibility and comparability of results. J. Paleolimnol. 25, 101–110.

Hoffman, J.S., Carlson, A.E., Winsor, K., Klinkhammer, G.P., LeGrande, A.N., Andrews, J.T., Strasser, J.C., 2012. Linking the 8.2 ka event and its freshwater forcing in the Labrador Sea. Geophys. Res. Lett. 39.

Hughes, P.D.M., Blundell, A., Charman, D.J., Bartlett, S., JDaniell, J.R.G., Wojatschke, A., Chambers, F.M., 2006. An 8500 cal. Year multi-proxy climate record from a bog in eastern Newfoundland: contributions of meltwater discharge and solar forcing. Quat. Sci. Rev. 25, 1208–1227.

Hurrell, J.W., Deser, C., 2009. North Atlantic climate variability: the role of the North Atlantic oscillation. J. Mar. Syst. 79, 231–244.

Kaplan, M.R., Wolfe, A.P., 2006. Spatial and temporal variability of Holocene temperature in the North Atlantic region. Quat. Res. 65, 223–231.

Keigwin, L.D., Sachs, J.P., Rosenthal, Y., Boyle, E.A., 2005. The 8200 year BP event in the slope water system, western subpolar North Atlantic. Paleoceanography 20.

Kelts, K., Hsu, K.J., 1978. Freshwater Carbonate Sedimentation. In: Lerman, A. (Ed.), Lakes: Chemistry, Geology, Physics. Springer-Verlag Berlin Heidelberg, Berlin, pp. 295–323.

Kim, S.T., O'Neil, J.R., 1997. Equilibrium and nonequilibrium oxygen isotope effects in synthetic carbonates. Geochim. Cosmochim. Acta 61, 3461–3475.

Kirby, M.E., Mullins, H.T., Patterson, W.P., Burnett, A.W., 2002. Late glacial-Holocene atmospheric circulation and precipitation in the Northeast United States inferred from modern calibrated stable oxygen and carbon isotopes. Geol. Soc. Am. Bull. 114, 1326–1340.

Laskar, J., Robutel, P., Joutel, F., Gastineau, M., Correia, A.C.M., Levrard, B., 2004. A long-term numerical solution for the insolation quantities of the earth. Astron. Astrophys. 428, 261–285.

Li, H.C., Ku, T.L., 1997. δ13C-δ18O covariance as a paleohydrological indicator for closed-basin lakes. Palaeogeogr. Palaeoclimatol. Palaeoecol. 133, 69–80.

Liu, Z., Yoshimura, K., Bowen, G.J., Buenning, N.H., Risi, C., Welker, J.M., Yuan, F., 2014. Paired oxygen isotope records reveal modern north American atmospheric dynamics during the Holocene. Nat. Commun. 5, 3701.

Liverman, D., Taylor, D., 1990. Surficial Geology Map of Insular Newfoundland, Report 90–1 Ed. Newfoundland Department of Mines and Energy, Geological Survey.

MacPherson, J.B., 1995. A 6 ka BP reconstruction for the island of Newfoundland from a synthesis of Holocene Lake sediment pollen records. Géog. Phys. Quatern. 49, 163–182.

Milrad, S.M., Atallah, E.H., Gyakum, J.R., 2010. Synoptic typing of extreme cool-season precipitation events at St. John's, Newfoundland, 1979–2005. Weather Forecast. 25, 562−+.

NGRIP, M., 2004. High-resolution record of northern hemisphere climate extending into the last interglacial period. Nature 431, 147–151.

Reimer, P.J., Bard, E., Bayliss, A., Beck, J.W., Blackwell, P.G., Ramsey, C.B., Buck, C.E., Cheng, H., Edwards, R.L., Friedrich, M., Grootes, P.M., Guilderson, T.P., Haflidason, H., Hajdas, I., Hatte, C., Heaton, T.J., Hoffmann, D.L., Hogg, A.G., Hughen, K.A., Kaiser, K.F., Kromer, B., Manning, S.W., Niu, M., Reimer, R.W., Richards, D.A., Scott, E.M., Southon, J.R., Staff, R.A., Turney, C.S.M., van der Plicht, J., 2013. IntCAL13 and Marine13 Radiocarbon Age Calibration Curves 0-50,000 Years Cal BP. Radiocarbon 55, 1869–1887.

Rimbu, N., Lohmann, G., Lorenz, S.J., Kim, J.H., Schneider, R.R., 2004. Holocene climate variability as derived from alkenone sea surface temperature and coupled ocean-atmosphere model experiments. Clim. Dyn. 23, 215–227.

Roland, T.P., Caseldine, C.J., Charman, D.J., Turney, C.S.M., Amesbury, M.J., 2014. Was there a '4.2 ka event' in great Britain and Ireland? Evidence from the peatland record. Quat. Sci. Rev. 83, 11–27.

Rozanski, K., Araguasaraguas, L., Gonfiantini, R., 1992. Relation between long-term trends of O-18 isotope composition of precipitation and climate. Science 258, 981–985.

Sachs, J.P., 2007. Cooling of Northwest Atlantic slope waters during the Holocene. Geophys. Res. Lett. 34.

South, G.R., 1983. Biogeography and Ecology of the Island of Newfoundland. W. Junk Publishers, Boston.

Steinman, B.A., Abbott, M.B., 2013. Isotopic and hydrologic responses of small, closed lakes to climate variability: hydroclimate reconstructions from lake sediment oxygen isotope records and mass balance models. Geochim. Cosmochim. Acta 105, 342–359.

Steinman, B.A., Pompeani, D.P., Abbott, M.B., Ortiz, J.D., Stansell, N.D., Finkenbinder, M.S., Mihindukalasooriya, L., Hillman, A.L., 2016. Oxygen isotope records of Holocene climate variability in the Pacific northwest. Quat. Sci. Rev. 142, 40–60.

Steinman, B.A., Rosenmeier, M.F., Abbott, M.B., 2010. The isotopic and hydrologic response of small, closed-basin lakes to climate forcing from predictive models: simulations of stochastic and mean-state precipitation variations. Limnol. Oceanogr. 55, 2246–2261.

Tindall, J.C., Valdes, P.J., 2011. Modeling the 8.2 ka event using a coupled atmosphere-ocean GCM. Glob. Planet. Chang. 79, 312–321.

Tremblay, L.B., Mysak, L.A., Dyke, A.S., 1997. Evidence from driftwood records for century-to-millennial scale variations of the high latitude atmospheric circulation during the Holocene. Geophys. Res. Lett. 24, 2027–2030.

Ullah, W., 1992. Water Resources Atlas of Newfoundland. Water Resources Division, Government of Newfoundland and Labrador, St. John, Newfoundland.

Vinther, B.M., Buchardt, S.L., Clausen, H.B., Dahl-Jensen, D., Johnsen, S.J., Fisher, D.A., Koerner, R.M., Raynaud, D., Lipenkov, V., Andersen, K.K., Blunier, T., Rasmussen, S.O., Steffensen, J.P., Svensson, A.M., 2009. Holocene thinning of the Greenland ice sheet. Nature 461, 385–388.

Yu, S.-Y., Colman, S.M., Lowell, T.V., Milne, G.A., Fisher, T.G., Breckenridge, A., Boyd, M., Teller, J.T., 2010. Freshwater outburst from Lake superior as a trigger for the cold event 9300 Years ago. Science 328, 1262–1266.

Yu, Z.C., McAndrews, J.H., Eicher, U., 1997. Middle Holocene dry climate caused by change in atmospheric circulation patterns: evidence from lake levels and stable isotopes. Geology 25, 251–254.